PERFORMANCE IMPROVEMENT OF A PHOTOVOLTAIC GENERATOR POWERED DC MOTOR-PUMP SYSTEM BASED ON ARTIFICIAL NEURAL NETWORKS

Ahmed. M. Kassem

Control Technology Dep., Beni-Suef University, Egypt,
Email: Kassem_ahmed53@hotmail.com

This paper presents the optimization of a photovoltaic (PV) water pumping system using maximum power point tracking technique (MPPT). The optimization is suspended to reference optimal power. This optimization technique is developed to assure the optimum chopping ratio of buck-boost converter. The presented MPPT technique is used in photovoltaic water pumping system in order to optimize its efficiency. An adaptive controller with emphasis on Nonlinear Autoregressive Moving Average (NARMA) based on artificial neural networks approach is applied in order to optimize the duty ratio for PV maximum power at any irradiation level. In this application, an indirect data-based technique is taken, where a model of the plant is identified on the basis of input-output data and then used in the model-based design of a neural network controller. The proposed controller has the advantages of robustness, fast response and good performance. The PV generator DC motor pump system with the proposed controller has been tested through a step change in irradiation level. Simulation results show that accurate MPPT tracking performance of the proposed system has been achieved. Further, the performance of the proposed artificial neural network (ANN) controller is compared with a PID controller through simulation studies. Obtained results demonstrate the effectiveness and superiority of the proposed approach.

KEYWORDS: *photovoltaic; maximum power point tracking; drive systems; artificial neural network controller.*

NOMENCLATURE

D	Duty ratio	K_t	Torque constant
D_m	Maximum duty ratio	L_a	Armature inductance
E_a	DC motor armature voltage	P_{mot}	Motor input power
E_b	Back emf voltage	R_a	Armature resistance
E_{bm}	Maximum back emf voltage	R_{sg}	PV generator series resistance
I_a	DC motor armature current	V_g	PV generator voltage
I_g	PV generator current	V_{gm}	PV generator maximum voltage
I_{gm}	PV generator maximum current	T_L	Load torque
I_{phg}	Insulation photo current of the PV generator	***Greek Symbol***	
I_{og}	PV generator reverse saturation current	β	friction coefficient

J	moment of inertia	ω	Rotor shaft speed
K_b	back emf constant	ξ	Load torque constant

1. INTRODUCTION

Photovoltaic (PV) energy has increased interest in electrical power applications. It is crucial to operate the PV energy conversion systems near the maximum power point to increase the efficiency of the PV system. The current and power of the PV array depends on the array terminal operating voltage. In addition, the maximum power operating point varies with insolation level and temperature. Therefore, the tracking control of the maximum power point is a complicated problem. To overcome these problems, many tracking control strategies have been proposed such as perturb and observe [1,2], incremental conductance [3], parasitic capacitance [4], constant voltage [5], neural network [6-11] and fuzzy logic controller (FLC) [12–17]. Some applications need constant output voltage with suitable MPPT or constant output current [18-19]. These strategies have some disadvantages such as high cost, difficulty, complexity and instability. Also, In [6-8] and [11] the neural networks are used only for maximum power estimation while a different controller is used to adjust the inverter output. But in this proposed system the adaptive artificial neural network controller is used to adjust the inverter output and there is no any more controller else needed.

The general requirements for maximum power point tracking (MPPT) are simplicity and low cost, quick tracking under changing conditions, and small output power fluctuation. A more efficient method to solve this problem becomes crucially important.

In photovoltaic pumping system, maximum power transfer is expected between photovoltaic solar panel (PV) and pump motor at wide irradiance interval. If not, performance may drop to low values to be removed. If the load voltage and or current are controlled to be constant these lead to Maximum power decreases [18].

This paper proposes a method to operate the motor pumping system at the high available efficiency. That is by tracking the maximum power point using adaptive neural NARMA-L2 controller. The NARMA L2 neurocontroller was first trained to cancel both the nonlinearity and dynamic of the system. Then, it was reconfigured to become a controller. Once the NARMA L2 neurocontroller suppresses both the nonlinearlity and dynamic behaviour, the closed loop system becomes implicit algebraic relation between the input and the output. Consequently, the system is able to perfectly follow a smooth reference trajectory even it is generated in real-time. A photo sensor and maximum power point tracker algorithm are used to generate the controller reference power. Also, the principle different between the proposed method and any other tracking method is that the proposed method attempts to track and compute the maximum power and controls directly the extracted power from the PV to that computed value through ANN controller. While, any other method attempts to reach the maximum point by the knowledge of the voltage or the current corresponding to that optimum point.

In this work, The feasibility and effectiveness of the PV generator, pumping system together with the proposed ANN controller have been demonstrated through

computer simulations. Moreover, the proposed controller is compared with a conventional PID controller. Simulation results have proved that the proposed controller can give better overall performance.

2. SYSTEM DYNAMICS

The proposed isolated generation system mainly consists of PV generator, DC-DC buck-boost converter and a DC motor coupled to a centrifugal pump as shown in Fig. 1. In the following subsections, a mathematical model for each device is developed and they combined together to form the complete model, which is to be used in the controller design and simulation studies.
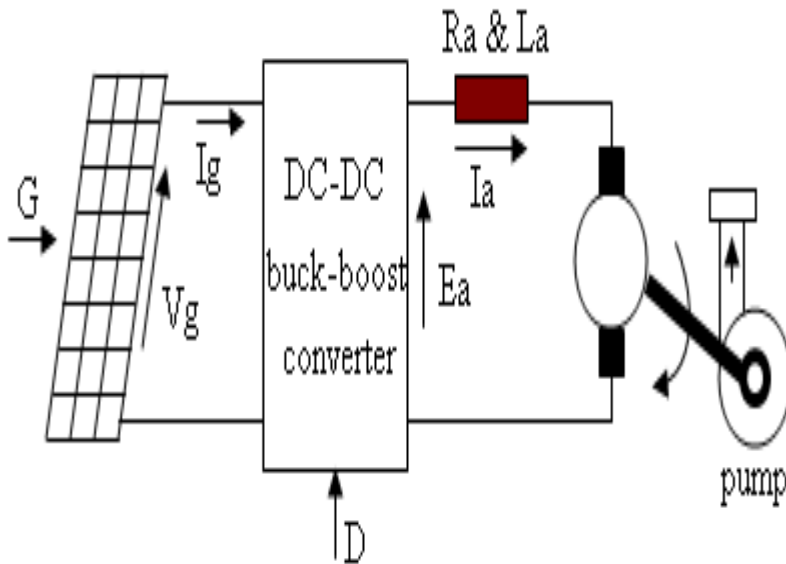
Fig. 1. The proposed PV-generator DC motor pump system

2.1 PV Generator Model

The PV generator consists of solar cells connected in series and parallel fashion to provide the desired voltage and current required by the DC motor system. This PV generator exhibits a nonlinear voltage-current characteristic that depends on the insulation (solar radiation), as given by (1) [20].

$$V_g = \frac{1}{A_g} \ln\left[\frac{GI_{phg} - I_g + I_{og}}{I_{og}}\right] - I_g R_{sg} \tag{1}$$

where V_g is the PV generator voltage; I_g is the PV generator current; $A_g = \Lambda/Ns$ is the PV generator constant; $\Lambda = q/(\varepsilon \times Z \times U)$, is the solar cell constant; $q = 1.602 \times 10^{-19}$ C. is the electron charge; $Z = 1.38 \times 10^{-23}$ J/K is Boltzman constant; $U = 298.15$ °C is the absolute temperature; $\varepsilon = 1.1$ is the completion factor; $Ns = 360$ is the series-connected solar cells; $N_p = 3$ is the parallel paths; $R_{sg} = R_s \times (N_s/N_p)$ is the PV generator series resistance; $R_s = 0.0152$ Ω is the series resistance per cell; $I_{phg} = I_{ph} \times N_p$ is the insulation-dependent photo current of the PV generator; $I_{ph} = 4.8$ A is the photo current per cell;

$I_{og}=I_o \times N_p$ is the PV generator reverse saturation current; $I_o=2.58e^{-5}$ A is the reverse saturation current per cell; G is the solar insulation in per unit, and 1.0 per unit of G = 1000 W/m^2.

The PV generator Voltage-Current and Voltage-Power characteristics at five different values of G are shown in Fig. 2. and Fig. 3 respectively. From which, at any particular value of G, there is only one point at which the PV generator power is maximum. This point is called the Maximum Power Point (MPP). To locate its position, the corresponding voltage (V_{gm}) and current (I_{gm}) must be determined first
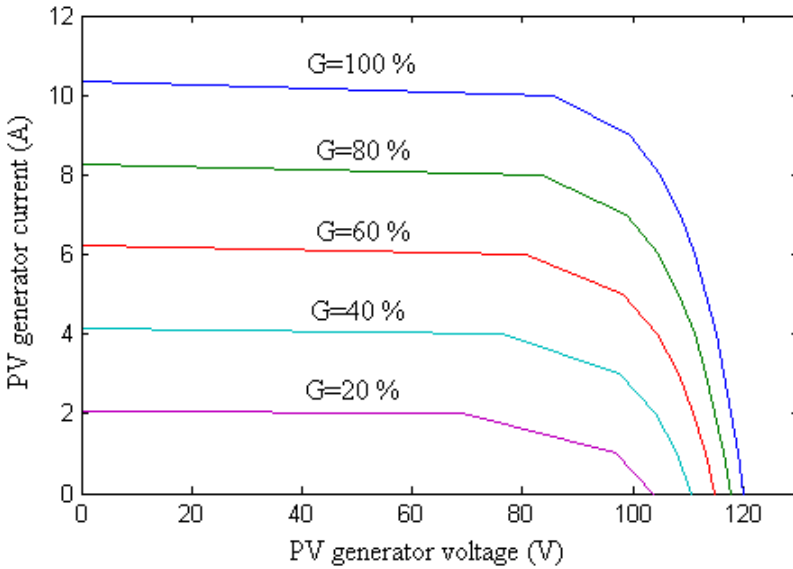
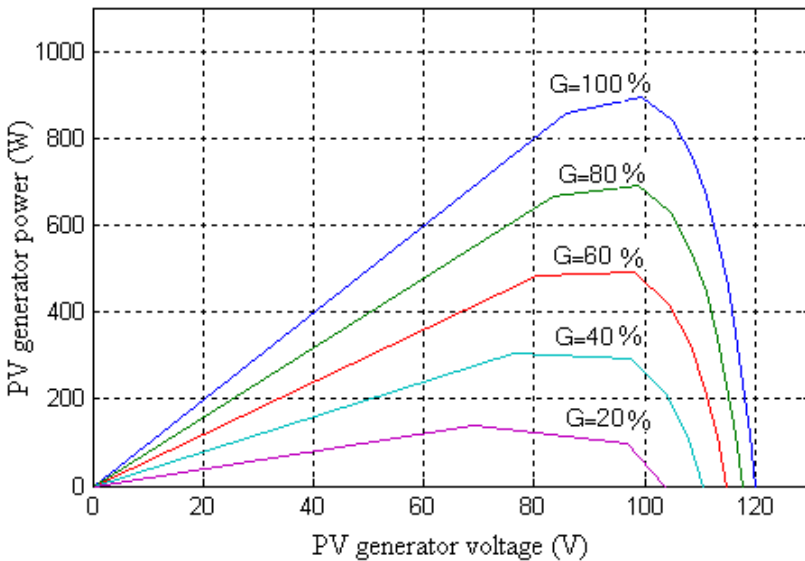Fig. 2. I-V characteristics of the PV generator at five different values of *G*.

Fig. 3. P-V characteristics of the PV generator at five different values of *G*.

2.2 DC Motor Model

The dynamics of the separately excited DC motor and its load are represented by the following set of differential equations with constant coefficients:

$$E_a = R_a I_a + L_a \frac{dI_a}{dt} + K_b \omega \tag{2}$$

$$K_t I_a = A_1 + \beta w + J \frac{d\omega}{dt} + T_L \tag{3}$$

The Load (pump) torque can be represented by:

$$T_L = A_2 + \xi \omega^{1.8} \tag{4}$$

where the name-plate parameters are: Voltage E_a=110 volt; Current I_a = 7.3 A.; Inertia J = 0.02365 Kg.m^2; Resistance R_a=1.5 Ω; Inductance La=0.2 H; Torque & back emf constant K =0.67609 Nm.A^{-1}; Motor friction A_1=0.2 Nm; Load friction A_2 = 0.3 Nm; damping coefficient B=0.002387 Nm.s.rad^{-1}; Load torque constant ξ = 0.00059 Nm.s.rad^{-1}.

2.3 DC-DC Converter Model

The most important parameter of the buck-boost converter is its chopping ratio Y that depends on the duty ratio D through a nonlinear relation given by:

$$Y = \frac{D}{1-D} \tag{5}$$

This converter is inserted between the PV generator and the DC motor to match the PV generator output characteristics to the DC motor input characteristics. Assuming the converter is ideal, then its input and output powers are equal resulting in the following relation [21]:

$$\frac{E_a}{V_{gm}} = \frac{I_{gm}}{I_a} = \frac{D}{1-D} \tag{6}$$

2.4 Power Regulator Model and MPPT Algorithm

There is a unique point on the PV voltage-current (I-V) and voltage-power (V-P) characteristic curves as shown in figures (2) and (3) respectively, called the maximum power point (MPP), at which the array produces maximum output power for each G. In general, when the load is direct-coupled, the operation point is not at the PV array's MPP, resulting an oversized PV array. However, because of the small scale of a PV array (less than 200 W), the over-sizing is cheaper than a commercial MPPT. But if the PV scale became more than 200 W, it will be preferable to operate it at the MPPT and with an economical method.

In this paper we chose a very simple method for MPPT operation, that by on-line estimating the PV maximum power output for each insulation level. However, we measure on-line the insulation level using photo sensor. Then we estimate the maximum power for each insulation level related to the following reference power equation:

$$P_{ref} = 205 - 1429.167\,G + 7208.33\,G^2 - 9270.833\,G^3 + 4166.67\,G^4 \tag{7}$$

The power output of the PV generator (delivered to the motor pump system) can be adjusted via controlling the duty ratio of the DC-DC converter according to the following differential equation:

$$\frac{dD}{dt} = P_{ref} - P_{mot} \tag{8}$$

Where $\quad P_{mot} = I_a E_a$

2.5 Complete System Model

The subsystem models can be interfaced to form the unified nonlinear model. The complete nonlinear dynamic model of the PV generator motor pump system can be described as:

$$\frac{dI_a}{dt} = \frac{1}{L_a} E_a - \frac{R_a}{L_a} I_a - \frac{K_b}{L_a} \omega \tag{9}$$

$$\frac{d\omega}{dt} = \frac{K_t}{J} I_a - \frac{A_1}{J} - \frac{\beta}{J} w - \frac{1}{J}\left(A_2 + \xi\omega^{1.8}\right) \tag{10}$$

$$\frac{dD}{dt} = P_{ref} - P_{mot} \tag{11}$$

Where

$$I_a = \frac{1-D}{D} I_g$$

$$E_a = \frac{D}{1-D} V_g = \frac{D}{1-D}\left\{ \frac{1}{A_g}\ln\left[\frac{GI_{phg} - I_g + I_{og}}{I_{og}}\right] - I_g R_{sg} \right\}$$

2.6 Linearized Model

Small signal linear model of the solar motor-pumped system is formed around an operating point to study the system dynamics when subjected to small perturbations. The linearized model can be described by the following equation:

$$px = Ax + B\mu + \delta d \tag{12}$$

Where
$x = [\Delta I_a \ \ \Delta\omega \ \ \Delta D]$, $\mu = [P_{ref}]$, $d = [G]$, and

A is a 3 x 3 matrix containing the system parameters.

3. MPPT CONDITION

For tracking maximum power points of PV with dc motor, system uses a dc/dc converter. This converter may be buck, boost or buck-boost type in respect of normal (direct coupled) operating characteristic of PV- pump motor. In this work, a buck-boost DC-DC converter is used. Assuming power converter is ideal, all of PV power is delivered to motor. Under MPPT conditions, motor is driven by maximum power of PV.

$$E_a I_a = V_{gm} I_{gm} \tag{13}$$

Motor input characteristics are defined by chopper ratio (D) of dc/dc converter. For maximum power tracking, there is a critical value of D with respect to a given irradiance level (D=D_m). Hence motor input voltage and current expressions:

$$E_a = \frac{D_m}{1 - D_m} V_{gm} \tag{14}$$

$$I_a = \frac{1 - D_m}{D_m} I_{gm} \tag{15}$$

In order to determine D_m, the steady-state equations of DC motor-Pump system can be written as follows:

$$E_a = I_a R_a + K \omega \tag{16}$$

$$E_b = K \omega \tag{17}$$

$$T = K I_a = A_2 + \xi \omega^{1.8} \tag{18}$$

$$P_{mech} = E_a I_a - I_a^2 R_a = T\omega \tag{19}$$

For a given G, the maximum power (P_m) is equal to maximum of $V_{gm}*I_{gm}$ values. At maximum power condition, the current is I_{gm}, voltage is V_{gm}. Hence as a function of G, P_m is;

$$P_m(G) = V_{gm}(G) I_{gm}(G) \tag{20}$$

Using equations (14-20) firstly shaft speed ω_m and back emf E_{bm} at maximum power are calculated for a given G (irradiance). These values also depend on pump load.

When motor input values (current and voltage) are transformed to PV side by use of D_m, the following equation is obtained:

$$(V_{gm} - R_a) D_m^2 + (I_{gm} R_a + R_a) D - (I_{gm} R_a + E_{bm}) = 0 \tag{21}$$

The positive root of equation (21) is equal to D_m. Hence using equations (14,15) motor input values are obtained. And then performance can be analyzed under MPPT condition. For normal system without MPPT, PV output current and voltage values are equal to those of motor input.

For analysis, PV pumping system is simulated based on Matlab/Simulink program environment. These results are shown by figs 4-6. For the average mechanical power at sampled irradiance levels, PV system with MPPT improves the system performance compared to normal system. Motor input power ($P_{mot}=E_a.I_a$) matches to PV maximum power point for overall irradiance levels.

Also using MPPT, higher speed and torque are provided at same irradiance conditions. Assuming least operating torque of system is equal to 2 Nm, normal system must wait until irradiance gets to 0.4 pu. Whereas for system with MPPT, approximately 0.2 pu irradiance level is sufficient to actively operate the system. Thus active operating region of pumping system is expanded by MPPT.
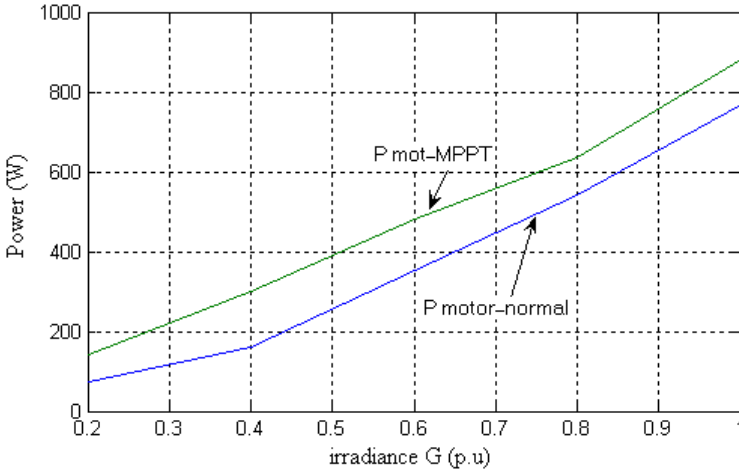
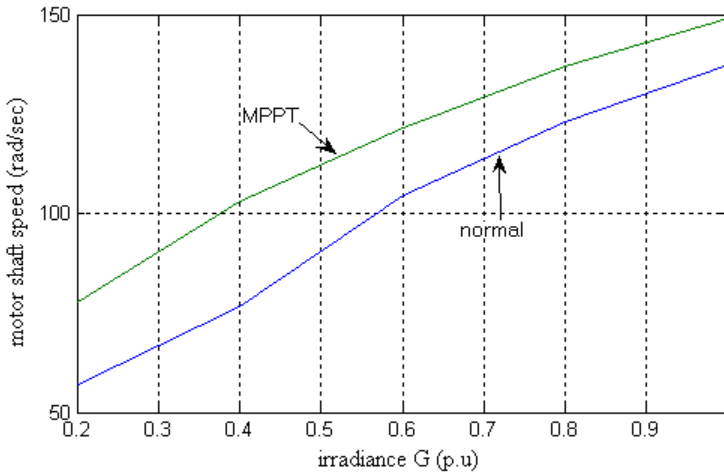Fig. 4: power versus G irradiance with and without MPPT

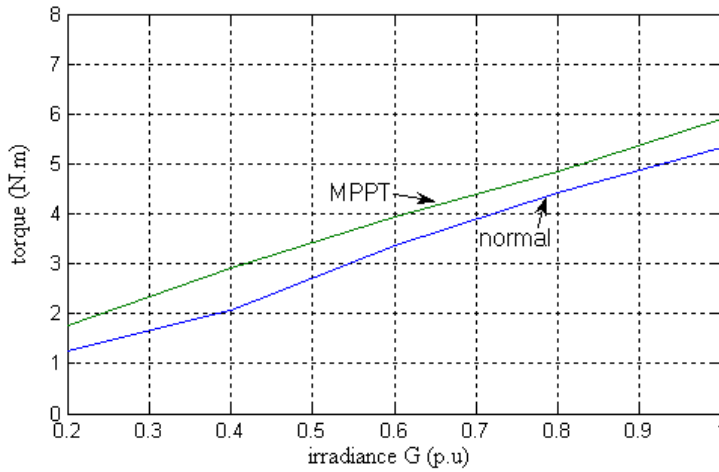Fig. 5: shaft speed versus G irradiance with and without MPPT

Fig. 6: torque versus G irradiance with and without MPPT

4. NONLINEAR AUTOREGRESSIVE MOVING AVERAGE (NARMA-L2) CONTROLLER

NARMA-L2 is one of the popular neural network architectures for prediction and control. The principle idea of this control scheme is to apply the input output linearization method where the output becomes a linear function of a new control input [22].

Basically, there are two steps involved when using NARMA L2 control: system identification and control design. In the system identification stage design, a neural network of the plant that needs to be controlled is developed using two subnetworks for the model approximation. The network is then trained offline in batch form using data collected from the operation of the plant. Next, the controller is simply the rearrangement of two subnetworks of the plant model. Computation of the next control input to force the plant output to follow a reference signal is materialized through simple mathematical equation.

4.1 NARMA-L2 Plant Model Identification

In this work, the ANN architecture is applied with the aid of the Neural Network Toolbox of MATLAB software. The identification can be summarized by the flowing:

The model structure used is the standard NARMA model [20] adapted to the feedback linearization of affine system. A companion form system (control affine) is used as the identification model, i.e.:

$$y(k+1) = f\begin{bmatrix} y(k), y(k-1),...,y(k-n+1), u(k-1) \\ ,...,u(k-m+1) \end{bmatrix} + g\begin{bmatrix} y(k), y(k-1),...,y(k-n+1), u(k-1) \\ ,...,u(k-m+1) \end{bmatrix} . u(k) \qquad (22)$$

In essence, the NARMA-L2 approximate model will be parameterized by two neural networks $\hat{f}$ and $\hat{g}$ that will be used to identify the system of Eq. (22), i.e.:

$$\hat{y}(k+1|\theta) = \hat{f}\begin{bmatrix} y(k), y(k-1),...,y(k-n+1), u(k-1) \\ ,...,u(k-m+1), w \end{bmatrix} + \hat{g}\begin{bmatrix} y(k), y(k-1),...,y(k-n+1), u(k-1) \\ ,...,u(k-m+1), v \end{bmatrix} . u(k) \qquad (23)$$

The two subnetworks are used for the model approximation; the first multilayer neural network (MLNN1) and the second multilayer neural network (MLNN2) , which are used to approximate nonlinear functions f and g respectively.

The plant model identification in NARMA-L2 Control starts off with a dataset of input output data pairs collected using the plant mathematical model. Then, the neural nets model is trained and validated. Here, the MLNN1 subnetwork is a feedforward neural network with five hidden layer with p neurons of hyperbolic tangent (tanh) activation function and an output layer of one neuron with linear activation function. Also, the MLNN2 subnetwork is a feedforward neural network with q tanh hidden layer neurons and one output neuron.

For each subnetwork, the number of past output n and the past input m; which compose the input vector and the number of neurons (p and q) of the hidden layer are determined. Subsequently, the selected neural network structure is trained using the input pattern and the desired output from the dataset. Here, the parameters

(weights and biases) of the two MLNN subnetworks that properly approximate the nonlinear modeling representing the optimized PV motor pump system power regulator is estimated.

Finally, to measure the success at approximating the dynamical system plant model using the neural network model, the prediction error e_k should be uncorrelated with all linear and nonlinear combination of past inputs and outputs. Thus, the validation and cross validation tests are carried out to ascertain the validity of the obtained neural network model [23-24].

4.2. NARMA-L2 Controller Design

There are two neural networks are used which are called f and g. Each one is a feed forward with three layers, i.e., an input, a hidden and an output layers. The input layer of f network has two nodes for the output power and a bias signal of 1.0. The input layer of g network has two nodes for the duty ratio and a bias signal of 1.0. The hidden layer has three nodes. The output layer has only one node. The output signal represents the duty ratio signal for the maximum power point.

The NARMA-L2 controller design is uncomplicated. The control action can be simply implemented using the obtained NARMA-L2 model based on Eq. 23 in which the functions f and g are defined. In order that a system output, y(k+1), to follow a reference trajectory $y_r(k+1)$, we set: y(k+1) = y_r(k+1). The NARMA-L2 controller is designed through substituting y(k+1) with y_r(k+1) in Eq. 23. Then the resolving controller output would have the form of:

$$u(k) = \frac{y_r(k+1) - \hat{f}\left[y(k), y(k-1), ..., y(k-n+1), u(k-1), ..., u(k-m+1)\right]}{\hat{g}\left[y(k), y(k-1), ..., y(k-n+1), u(k-1), ..., u(k-m+1)\right]} \tag{24}$$

Figure 7 shows the block diagram of NARMA-L2 controller which clearly a rearrangement of the NARMA-L2 plant approximated model.
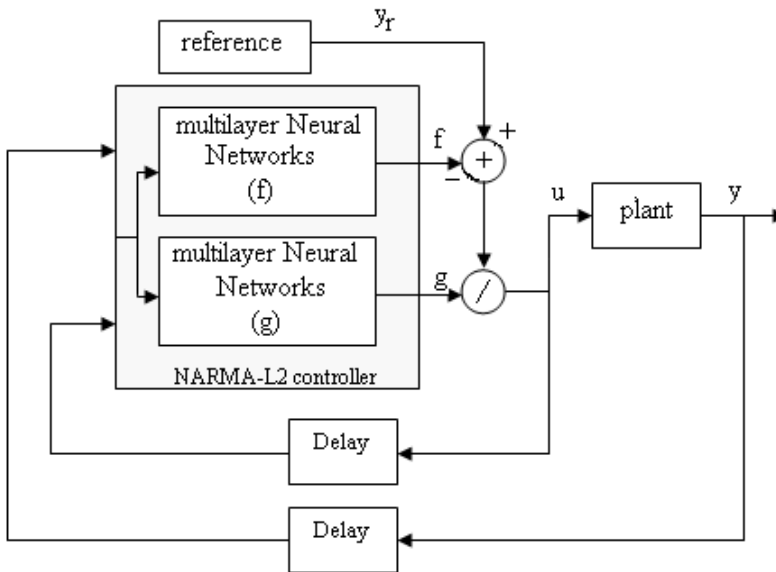

Fig. 7: NARMA-L2 controller schematic.

5. SYSTEM CONFIGURATION

The main objectives of the proposed NARMA controller are to track and extract the maximum available power from PV generator feeding motor pump system. That is done by adjusting the suitable value of the duty ratio to give the maximum power. The NARMA controller output signal D is given by:

$$D(k) = \frac{\hat{P}_{ref}(k+1) - \hat{f}\left[P_a(k), P_a(k-1),..., P_a(k-n+1), D(k), D(k-1),..., D(k-m+1)\right]}{\hat{g}\left[P_a(k), P_a(k-1),..., P_a(k-n+1), D(k), D(k-1),..., D(k-m+1)\right]D(k+1)} \quad (25)$$

The block diagram of the PV generator motor-pump system with the MPPT algorithm and the proposed NARMA controller is shown in Fig. 8. The entire system has been simulated on the digital computer using the neural networks tool box in Matlab/Simulink [25] software package.
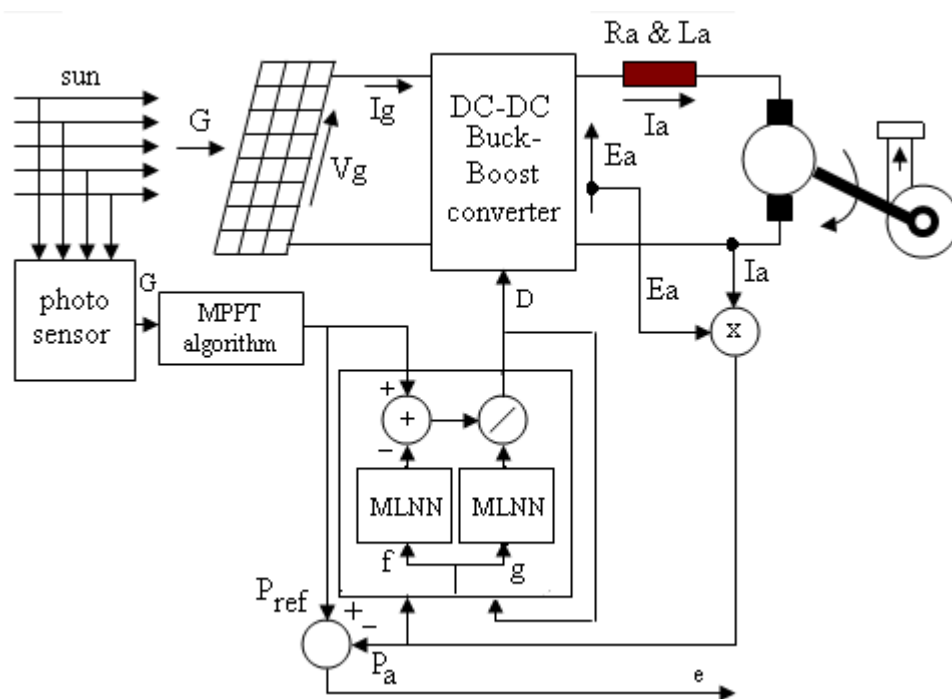

Fig. (8): Block diagram of the PV generator motor-pump system with the MPPT algorithm and the proposed ANN controller.

6. SIMULATION RESULTS

Computer simulations have been carried out in order to validate the effectiveness of the proposed scheme. As mentioned previously the Neural networks are trained offline and in batch form. We have used 5 hidden layers and 10000 sample data, which are generated to train the network. 100 training epochs and employing training as a training function were enough to get good results. The training, validation and testing data of the ANN controller are shown in Figs 9, 10 and 11 respectively. The performance of the proposed system has been tested with a step change in solar

insulation level. Thus, the solar insulation level assumed to vary abruptly between 400 W/m^2 and 800 W/m^2 as shown in fig. 12, which mean that the reference maximum power vary also abruptly between 480 watts and 635 as shown in fig. 13. Figs. 13-17 illustrate the dynamic responses of the actual and reference power, armature current, shaft speed, duty ratio and armature voltage respectively for both PID controller and the proposed ANN controller.

It has been noticed in the figs 13-17 that as the solar insulation level increases from 600 W/m^2 to 800 W/m^2, the power output of the PV-generator (reference power) will increase related to the maximum power algorithm, the duty ratio will increase such that the output power of the DC-DC converter equal the PV-generator maximum power, also both armature current and voltage will increase to meet the increasing in power and by the way the motor shaft speed will increase. And vice versa if the solar insulation level decreases. The response of the ANN controller is compared with the PID one for the same conditions. Tuning of the PID controller was done by trial and error. In addition, these figures show that the power delivered to the motor-pump system follow the PV maximum output power with small settling time and with zero steady state error. Also these figures indicate that the dynamic responses based on the proposed ANN controller is better than the conventional PID controller in terms of fast response and small maximum overshoot.

Simulation results show also that a motor pump system can be supplied from a PV-generator with the maximum available power, which is needed by the load.

7. CONCLUSIONS

In this study, the ANN controller has been used in order to design a state feedback static controller for a PV pumping system. The controlled system consists of a PV generator that supplies a DC motor pump system through buck-boost DC-DC converter. The control objective aims to track and operate the motor-pump system at the MPPT of the PV generator. This is carried out via controlling the duty ratio of the DC-DC converter. The results show that the MPPT techniques add about 38% more performance than at normal condition. The results also show that the maximum power tracker is achieved with zero steady state error and with settling time less than one second and accurate tracking performance of the proposed system has been achieved. Also the results show that the proposed ANN controller has significantly better performance than the classical PID controller.
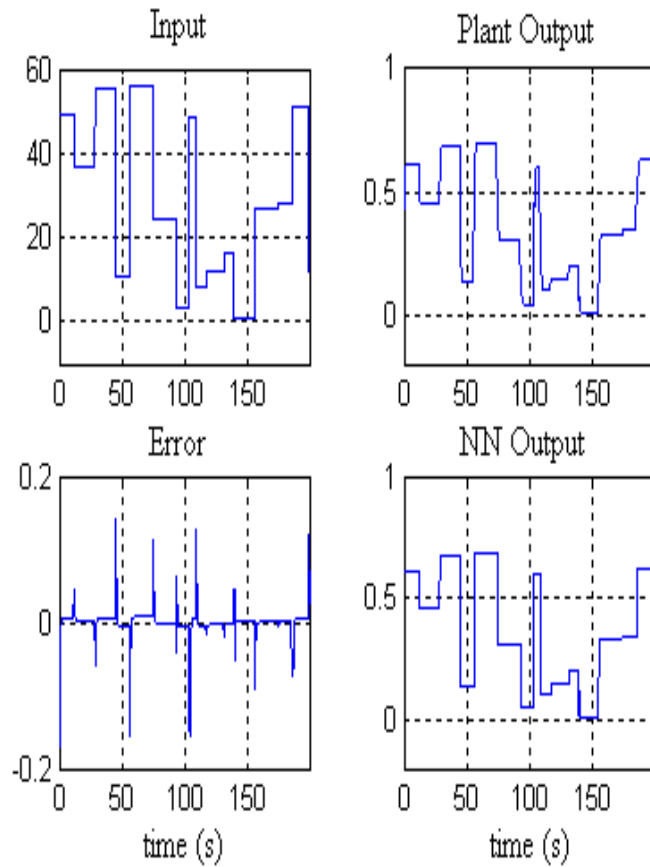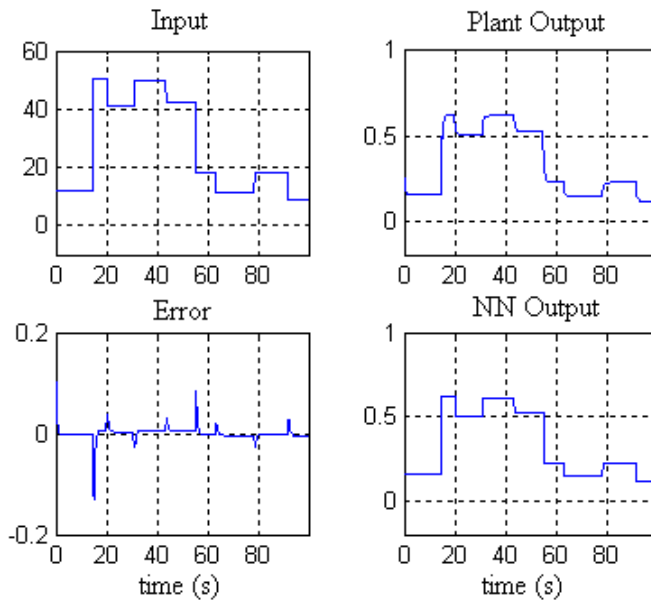
Fig. 9: Training data of ANN controller

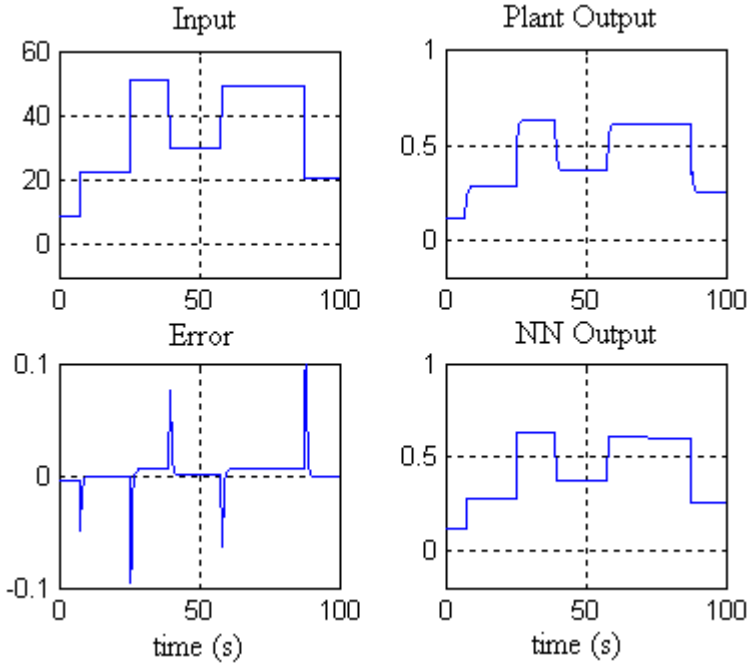Fig. 10: Validation data of ANN controller
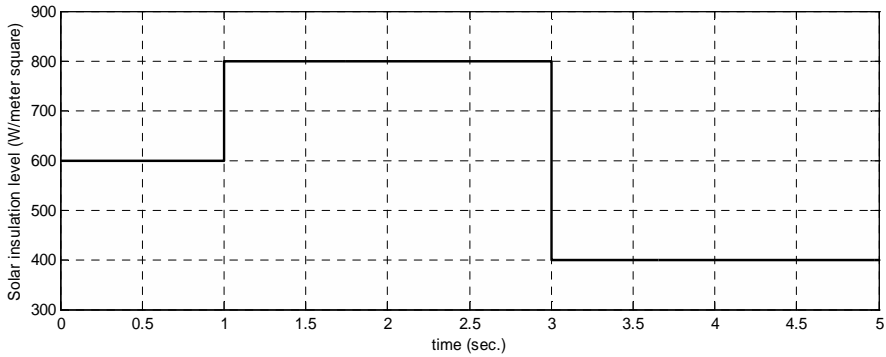
Fig. 11: testing data of ANN controller.

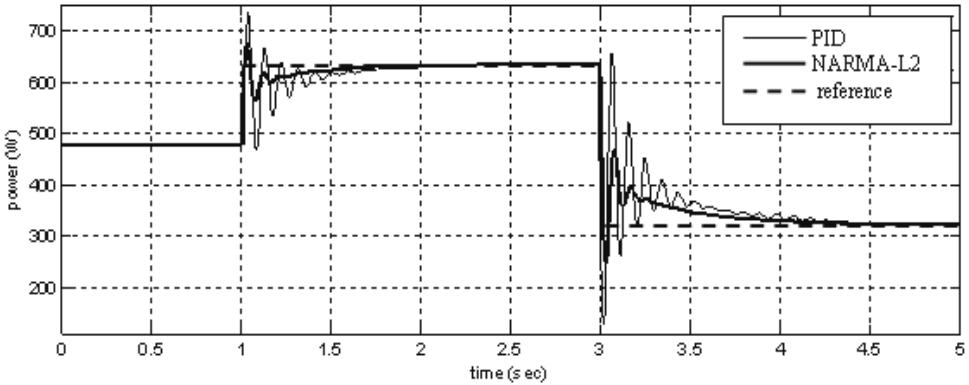Fig. 12: Solar insulation level variations.

Fig. 13: Dynamic responses of power due to step change in the insulation level.
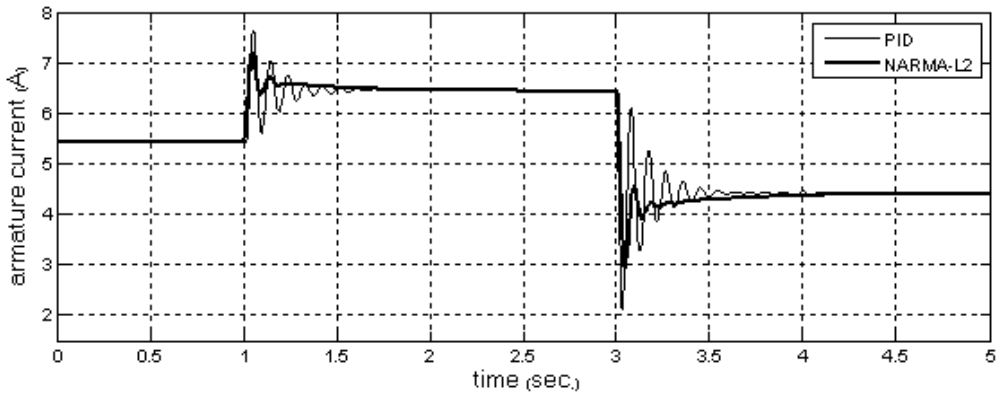
Fig. 14: Dynamic responses of armature current due to step change in the insulation level.
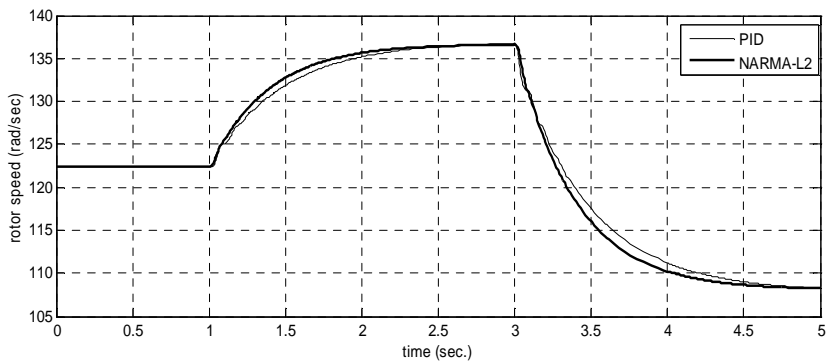
Fig. 15: Dynamic responses of rotor speed due to step change in the insulation level.
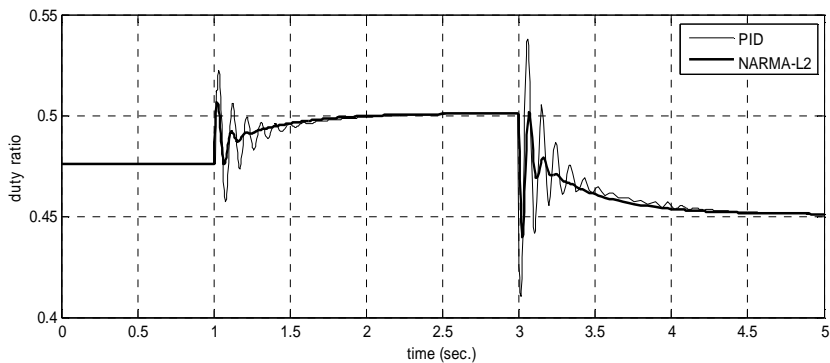
Fig. 16: Dynamic responses of duty ratio due to step change in the insulation level.
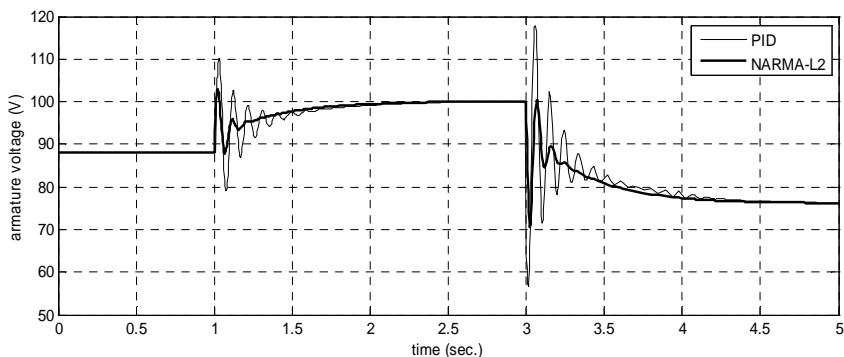
Fig. 17: Dynamic responses of armature voltage due to step change in the insulation level.

REFERENCES

[1] Hua C, Shen C. "Comparative study of peak power tracking techniques for solar storage system". IEEE Appl. Power Electron Conf. Exposition Proc., 1998.

[2] Hussein KH, Muta I, Hoshino T, Osakada M., "Maximum photovoltaic power tracking: an algorithm for rapidly changing atmospheric conditions". IEEE Proc. Generation Transmission Distribution, pp 59-64, 1995.

[3] Brambilla A., "New approach to photovoltaic arrays maximum power point tracking". Proc 30th IEEE Power Electron. Specialists Conf., 1998.

[4] Hohm DP, Ropp ME., "Comparative study of maximum power point tracking algorithm using an experimental, programmable, maximum power point tracking test bed". Proc. 28th IEEE Photovoltaic Specialist Conf., 2000.

[5] Swiegers W, Enslin J., "An integrated maximum power point tracker for photovoltaic panels". Proc. IEEE Int. Symp. Ind. Electron., 1998.

[6] Hiyama T, Kitabayashi K., "Neural network based estimation of maximum power generation from PV module using environment information". IEEE Trans. On Energy Conversion, 1997.

[7] Hiyama T, Kouzuma S, Imakubo T, Ortmeyer TH., "Evaluation of neural network based real time maximum power tracking controller for PV system". IEEE Trans. On Energy Conversion, 1995.

[8] Hiyama T, Kouzuma S, Imakubo T., "Identification of optimal operating point of PV modules using neural network for real time maximum power tracking control". IEEE Trans. On Energy Conversion, 1995.

[9] Torres AM, Antunes FLM., "An artificial neural network-based real time maximum power tracking controller for connecting a PV system to the grid". Proc. Of IEEE Annu. Conf. in Ind. Electron., 1998.

[10] Al-Amoudi A, Zhang L., "Application of radial basis function networks for solar-array modeling and maximum power-point prediction". IEEE Proc— Generation Transmission Distribution, 2000.

[11] A.B.G. Bahgat, N.H. Helwa, G.E. Ahmad and E.T. El Shenawy, "Maximum power point traking controller for PV systems using neural networks". Renewable Energy, Vol. 30, No 8, pp 1257-1268 , 2005.

[12] Won CY, Kim DH, Kim SC, Kim WS, Kim HS., "A new maximum power point tracker of photovoltaic arrays using fuzzy controller". Proc. Of Annu. IEEE Power Electron. Specialists Conf., 1994.

[13] Senjyu T, Uezato K., "Maximum power point tracker using fuzzy control for photovoltaic arrays". Proc. Of IEEE Int. Conf. in Ind. Technol., 1994.

[14] Simoes MG, Franceschetti NN., "Fuzzy odeling ion based control of a solar array system". IEEE Proc. Of Electric Power Appl., 1999.

[15] Mahmoud AMA, Mashaly HM, Kandil SA, El Khashab H, Nashed MNF., "Fuzzy logic implementation for photovoltaic maximum power tracking". Proc. Of 9th IEEE Int. workshop Robot Human Interactive Commun, Osaka, Japan, 2000.

[16] Andouisi, R.; Mami, A.; Dauphin-Tanguy, G.; Annabi, M., " Bond graph odeling and dynamic study of a photovoltaic system using MPPT buck-boost converter". IEEE International Conference on Systems, Man and Cybernetics , Vol 3, No 6, oct., Tunisia, 2002.

[17] Hamrouni, N.; Jraidi, M.; Cherif, A.; Dhouib, A., " Measurements and Simulation of a PV Pumping Systems Parameters Using MPPT and PWM Control Strategies". IEEE Mediterranean Electrotechnical Conference (MELECON), Tunis, pp 885 – 888, May, 2006.

[18] Marcelo Gradella Villalva and Ernesto Ruppert Filho., " Dynamic Analysis Of The Input-Controlled Buck Converter Fed By A Photovoltaic Array". Revista Controle & Automação/Vol.19, No.4, 2008.

[19] Sachin Jain and Vivek Agarwal., "New current control based MPPT technique for single stage grid connected PV systems". Energy conversion and management, Vol 48, Issue 2, pp 625-644, 2007.

[20] Ahmed Hussein, Kotaro Hirasawa and Jinglu Hu., "A robust control method for a PV-supplied DC motor using universal learning networks". Solar Energy Journal, Vol. 76, pp 771-780, 2004.

[21] A. Saadi and A. Moussi, "optimization of buck-boost converter by MPPT Technique with a variable reference Voltage Applied to Photovoltaic Water Pumping System Under Variable Weather Conditions". Asian Journal of Info. Technology, Vol 6, No 2, pp 222-229, 2007.

[22] Awwad, A.; Abu-Rub, H.; Toliyat, H.A., "Nonlinear autoregressive moving average (narma-l2) controller for advanced AC motor control". IEEE Annual conference of Industrial Electronics, Erlangen, pp 1287-1292, Nov., 2008.

[23] Ali Al-Alawi, Saleh M Al-Alawi and Syed M Islam, "Predictive control of an integrated PV-diesel water and power supply system using an artificial neural network". Renewable Energy, Vol 32, No 8, pp 1426-1439, 2007.

[24] Yang Xu Zeng Chengbi, " Generalized Dynamic Fuzzy Neural Network-based Tracking Control of PV". IEEE Power and Energy Engineering Conference (APPEEC), pp 1-4, March 2010.

[25] H. Demuth , M. Beale, M. Hagan., "Neural network toolbox user's guide for use with MATLAB". Natick, MA: The Math Works, Inc., 2006.

تحسين أداء نظام مكون من مولد كهروضوئي يغذي مضخة مدارة بمحرك تيار مستمر باستخدام الشبكات العصبية الاصطناعية

تزايدت الاهتمامات في السنوات الأخيرة إلي استخدام الطاقة الجديدة والمتجددة في توليد الطاقة الكهربية وخاصة من الطاقة الشمسية كونها طاقة صديقة للبيئة واقتصادية ومتوفرة في معظم مناطق العالم. يتعرض هذا البحث إلي تقنية التحكم في تشغيل وتحسين كفاءة وحدة توليد كهربي من الطاقة الشمسية والحصول علي القيمة القصوى من الطاقة الكهربية المستخلصة من وحدة التوليد المقترحة. تستخدم وحدة توليد الكهرباء المقترحة لتغذية حمل بمنطقة نائية بعيدا عن مصادر الكهرباء التقليدية عبارة عن مضخة مياه مدارة بمحرك تيار مستمر. تم ربط المحرك الكهربي بوحدة التوليد الكهربي من خلال buck-boost converter. تم تصميم نظام تحكم يستند إلي استخدام (Nonlinear Autoregressive Moving Average controller) المعتمد علي تقنية الشبكات العصبية الاصطناعية (artificial neural networks) وذلك للتحكم في الجهد علي أطراف المحرك الكهربي وكذلك لاستخلاص اكبر قدرة ممكنة من وحدة توليد الطاقة الشمسية مما يحسن من كفاءة النظام. تم اختبار أداء النظام بالتغير الفجائي في مستوي الإشعاع (irradiation level). أيضا تم مقارنة أداء نظام التحكم المقترح (artificial neural networks) مع نظام تحكم تقليدي (PID) وأيضا مقارنة أداء الحاكم بتتبع إشارة القدرة القصوى المرجعية.